

## **Inventory of Supplementary Information**

**Supplementary Fig.1, related to Fig. 1.**

**MDH2 acetylation does not affect the GOT2-MDH2 association**

**Supplementary Fig.2, related to Fig. 1.**

**Fourteen putative acetylated lysine residues in the GOT2 protein**

**Supplementary Fig.3, related to Fig. 1.**

**The position of putative acetylated lysines in the structure of GOT2 protein**

**Supplementary Fig.4, related to Fig. 1.**

**Mapping the major lysine residue(s) of acetylation in GOT2 whose acetylation can affect GOT2-MDH2 association**

**Supplementary Fig.5, related to Fig. 1.**

**Characterization of the anti-acetyl-GOT2 (K159) antibody**

**Supplementary Fig.6, related to Fig. 2.**

**Both glucose and glutamine can increase the mitochondrial NADH level**

**Supplementary Fig.7, related to Fig. 2.**

**Identification of *GOT2* knocking-down and putting-back cell lines**

**Supplementary Fig.8, related to Fig. 4.**

***GOT2* knockdown impairs the net transfer of cytosolic NADH into mitochondria, suppresses cellular ATP and NADPH production, increases ROS, and inhibits cell growth**

**Supplementary Fig.9, related to Fig. 4.**

***NADK2* knockdown cannot block the antioxidant response in rescued cells expressing 3KQ mutant *GOT2***

**Supplementary Fig.10, related to Fig. 4.**

***GOT2* 3K acetylation affects cytosolic redox status in the cell**

**Supplementary Fig.11, related to Fig. 4.**

**GOT2 3K acetylation does not affect the activity of nuclear SIRT1 or cytosolic SIRT2**

**Supplementary Fig.12, related to Fig. 4.**

**GOT2 3K acetylation decreases basal respiration without affecting ATP turnover and respiration capacity in the cell**

**Supplementary Fig.13, related to Fig. 4.**

**GOT2 3K acetylation significantly increases glucose and glutamine uptake**

**Supplementary Fig.14, related to Fig. 4.**

**Overexpression of SIRT3, but not NMN treatment, suppresses pancreatic cancer cell proliferation**

**Supplementary Experimental Procedures**

**Supplementary Reference**

## Yang et al. Supplemental Figure 1

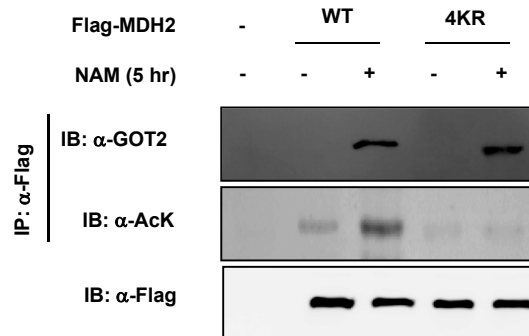


### Figure S1. MDH2 acetylation does not affect the GOT2-MDH2 association

Flag-tagged wild-type MDH2 and the acetylation-deficient 4KR mutant (i.e., K185, K301, K307, and K314) were transiently overexpressed in HEK293T cells, and the transfected cells were treated without or with NAM (5 mM) for 5 hrs. The protein association of wild-type or 4KR mutant MDH2 with endogenous GOT2 was determined by western blot analysis.



Yang et al. Supplemental Figure 3

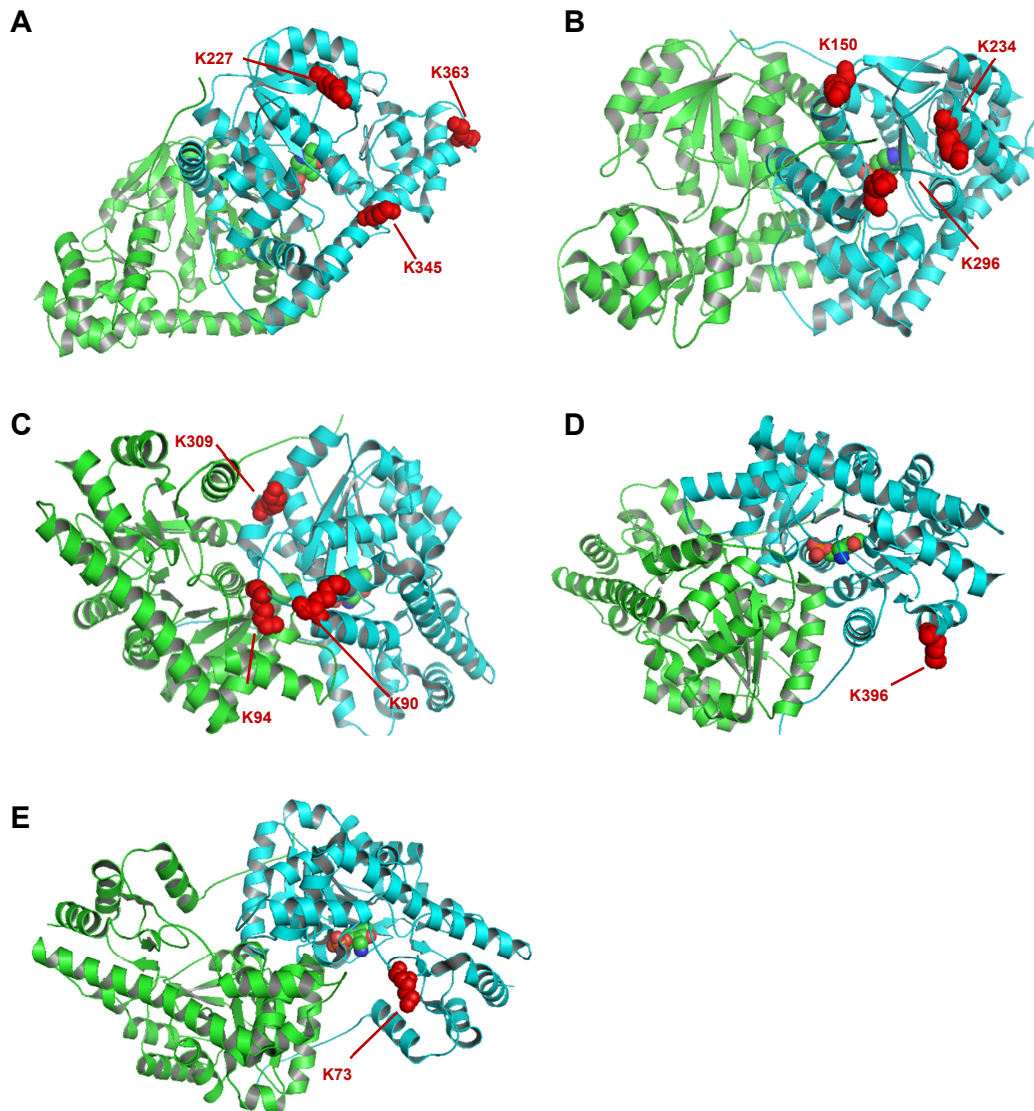


**Figure S3. The position of putative acetylated lysines in the structure of GOT2 protein**

Cartoon representation of the GOT2 structure (PDB ID: 3PDB) (Han et al. 2011) made by Pymol ([www.pymol.org](http://www.pymol.org)). The putative acetylated lysines were divided into 6 groups and were colored in red. Among them, 5 groups were shown in this figure. See also Figure 1G.

Yang et al. Supplemental Figure 4

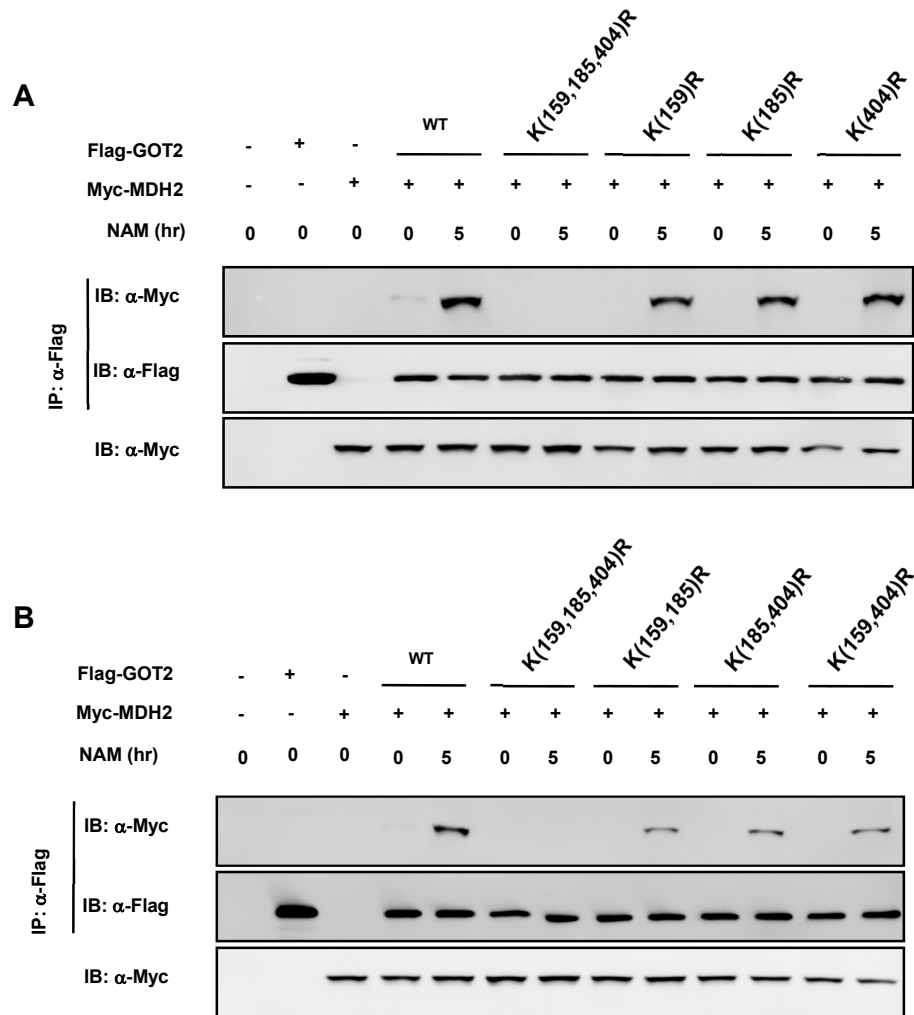


**Figure S4. Mapping the major lysine residue(s) of acetylation in GOT2 whose acetylation can affect GOT2-MDH2 association**

Myc-tagged MDH2 were co-overexpressed with single or double K to R mutation targeting K159, K185 or K404 in the GOT2 protein in HEK293T cells. The protein interaction between Myc-MDH2 and single **(A)** and double **(B)** GOT2 KR mutants was determined by western blot analysis.

# Yang et al. Supplemental Figure 5

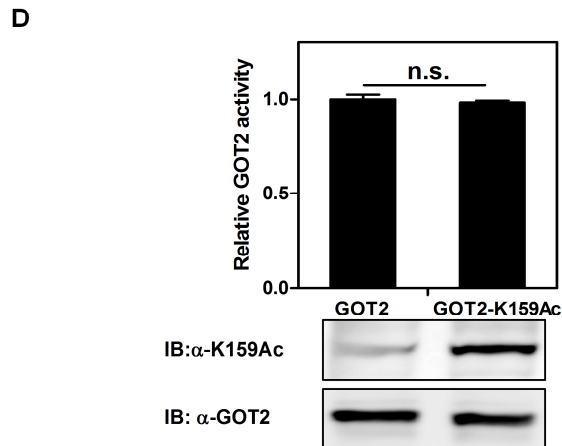
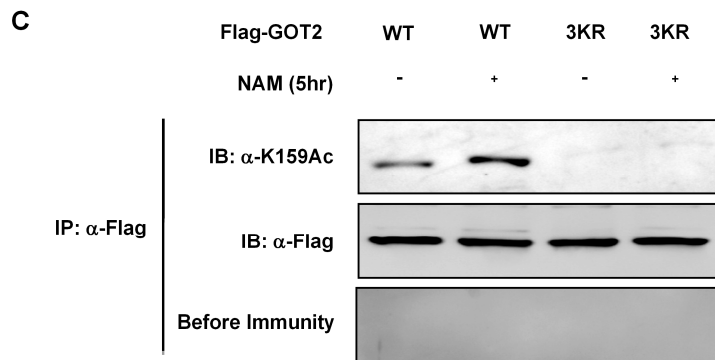
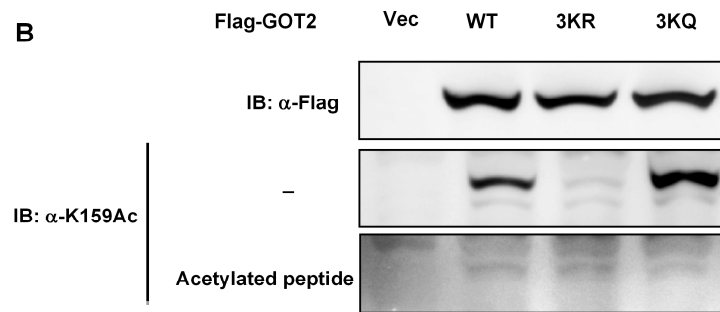
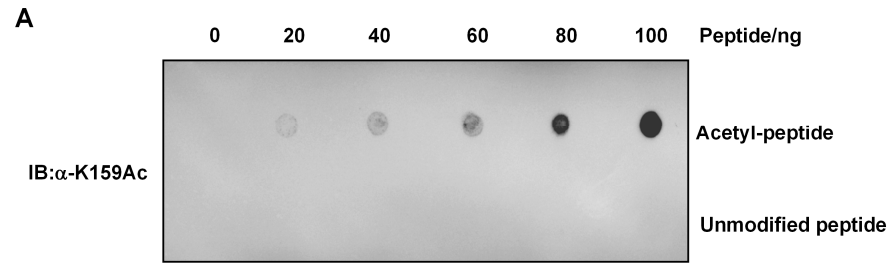


**Figure S5. Characterization of the anti-acetyl-GOT2 (K159) antibody**

**(A)** Different amounts of acetyl-K159 peptide or unmodified peptide were spotted on nitrocellulose membrane, and the antibody specificity was determined by dot-blot assay.

**(B)** Flag-tagged wild-type and 3KR/Q mutant GOT2 were overexpressed in HEK293T cells. Immunoprecipitated Flag-tagged wild-type GOT2 and its 3KQ mutant, but not 3KR mutant, was recognized by the  $\alpha$ -acGOT2(K159) antibody.

**(C)** Flag-tagged wild-type and 3KR mutant GOT2 were overexpressed in HEK293T cells treated without or with NAM (5 mM) for 5 hrs. Wild-type Flag-GOT2, but not its 3KR mutant, displayed an increase in the K159 acetylation level after NAM treatment.

**(D)** Recombinant un-acetylated and K159-acetylated GOT2 proteins were purified by the system of genetically encoding N<sup>ε</sup>-acetyllysine in *E. coli*. The activity and the K159 acetylation level of recombinant GOT2 proteins were determined by enzyme activity assay and western blot analysis, respectively.

Shown are average values with standard deviation (S.D.) of triplicated experiments. n.s.=not significant.



## Yang et al. Supplemental Figure 6

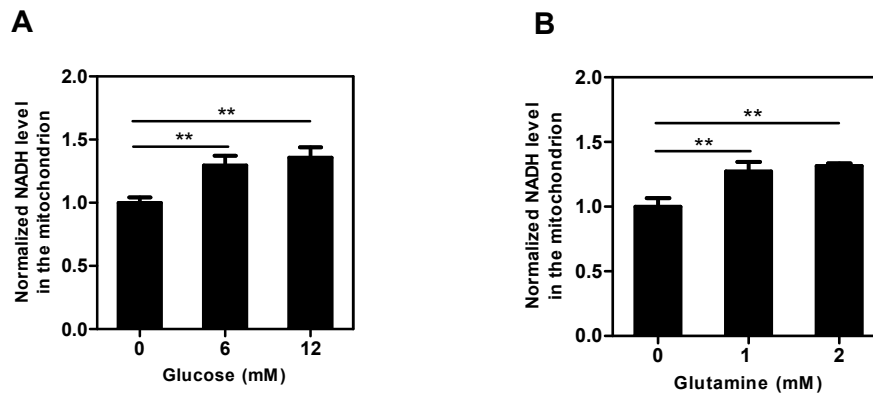


**Figure S6. Both glucose and glutamine can increase the mitochondrial NADH level**

Panc-1 cells were treated with increased concentrations of glucose (**A**) or glutamine (**B**) as indicated. The relative level of NADH in the mitochondrion was determined as described in “Method”. Shown are average values with standard deviation (S.D.) of triplicated experiments. \*\*denotes the  $p < 0.01$  for the indicated comparison.

## Yang et al. Supplemental Figure 7

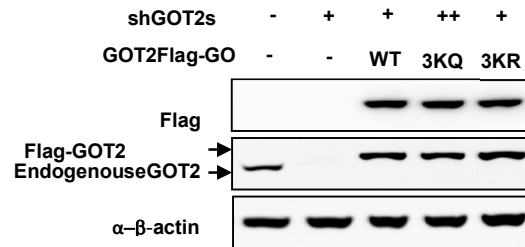


**Figure S7. Identification of *GOT2* knocking-down and putting-back cell lines**

Pan-1 cells with stable knockdown of endogenous *GOT2* were transfected with retroviral plasmids expressing the indicated proteins. The presence of ectopically expressed and endogenous proteins was verified by western blotting.

Yang et al. Supplemental Figure 8

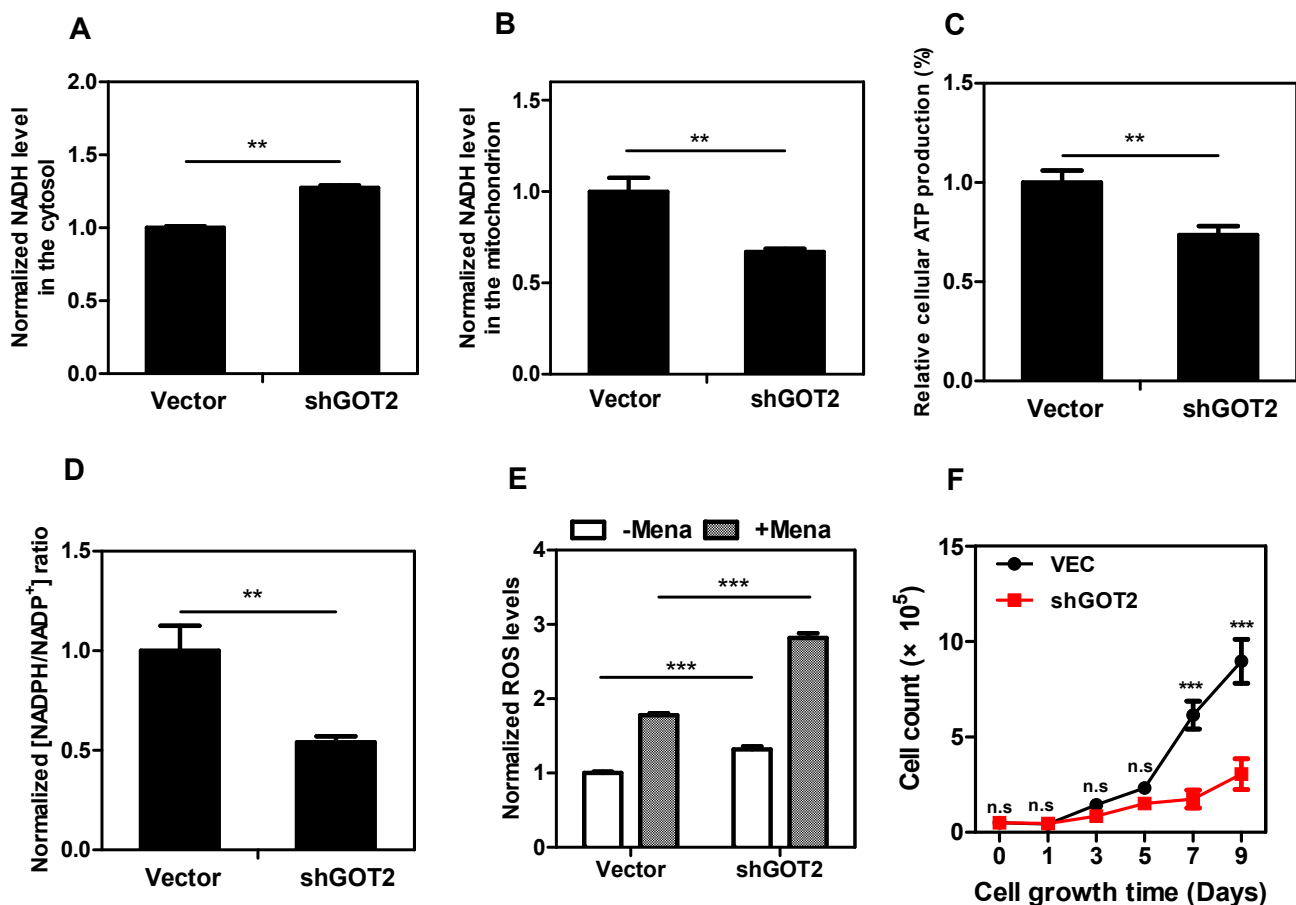


**Figure S8. *GOT2* knockdown impairs the net transfer of cytosolic NADH into mitochondria, suppresses cellular ATP and NADPH production, increases ROS, and inhibits cell growth**

**(A-B)** *GOT2* knockdown inhibits the net transfer of cytosolic NADH into mitochondria. In Panc-1 stable cells with *GOT2* knock-down and control cells expressing the empty vector, the NADH level in the cytosol **(A)** and mitochondrion **(B)** was determined in cell extracts as described in “Method”.

**(C)** *GOT2* knockdown inhibits ATP production. In Panc-1 stable cells with *GOT2* knock-down and control cells expressing the empty vector, ATP production was determined in cell extracts as described in “Method”.

**(D)** *GOT2* knockdown inhibits NADPH production. In Panc-1 stable cells with *GOT2* knock-down and control cells expressing the empty vector, the NADPH/NADP<sup>+</sup> ratio was determined in cell extracts as described in “Method”.

**(E)** *GOT2* knockdown increases cellular ROS levels. In Panc-1 stable cells with *GOT2* knock-down and control cells expressing the empty vector, ROS levels were determined in cells after treatment without or with menadione (50 μM for 30 min), as described in “Method”.

**(F)** *GOT2* knockdown decreases the growth rate of pancreatic cells in culture. Panc-1 stable cells with *GOT2* knock-down and control cells expressing the empty vector were seeded in a 6-well plate, and cell numbers were counted every 1-2 days over a period of 9 days.

Shown are average values with standard deviation (S.D.) of triplicated experiments. \*\*denotes the  $p < 0.01$  and \*\*\*denotes the  $p < 0.001$  for the indicated comparison; n.s.= not significant.

Yang et al. Supplemental Figure 9

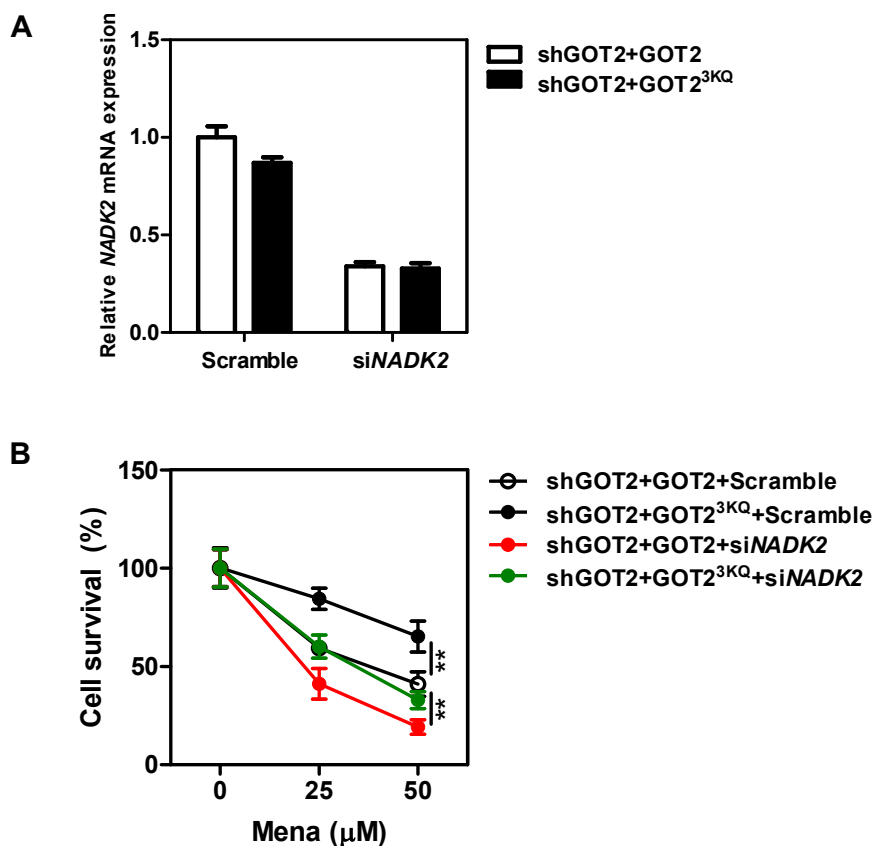


**Figure S9. *NADK2* knockdown cannot block the antioxidant response in rescued cells expressing 3KQ mutant GOT2**

**(A)** Panc-1 cells with *GOT2* knocking-down and putting-back were transfected with siRNA targeting the *NADK2* gene. The knockdown efficiency of *NADK2* was verified by qRT-PCR.

**(B)** Cells in (A) were treated with increased concentrations of menadione for 3 hrs as indicated. Cell viability was determined by counting the remaining adherent cells.

Shown are average values with standard deviation (S.D.) of triplicated experiments. \*\*denotes the  $p < 0.01$  for the indicated comparison.

Yang et al. Supplemental Figure 10

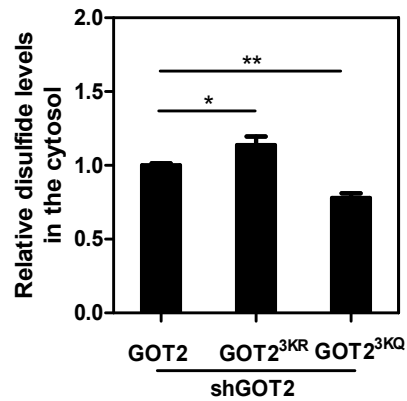


**Figure S10. GOT2 3K acetylation affects cytosolic redox status in the cell**

Panc-1 cells with *GOT2* knocking-down and putting-back were transfected with a retroviral plasmid expressing cytosolic redox-sensitive green fluorescent protein 1 (roGFP1). The disulfide level in the cytosol of living cells was determined as described in "Method". Shown are average values with standard deviation (S.D.) of triplicated experiments. \*denotes the  $p < 0.05$  and \*\*denotes the  $p < 0.01$  for the indicated comparisons.

Yang et al. Supplemental Figure 11

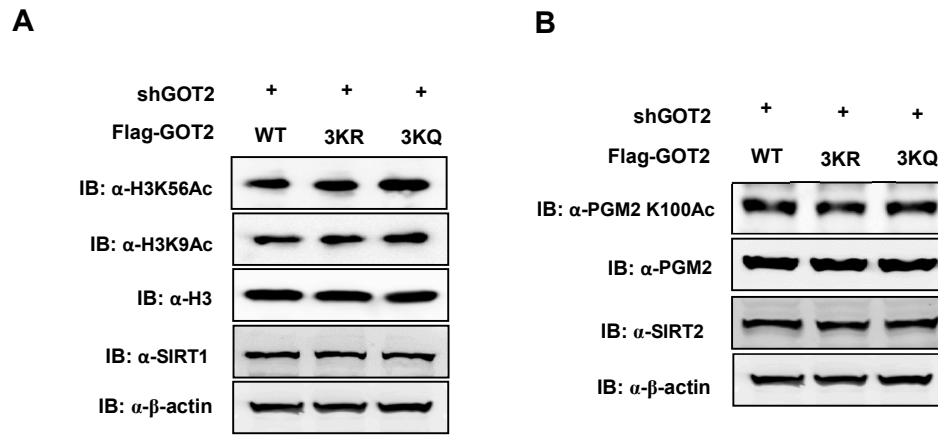


**Figure S11. GOT2 3K acetylation does not affect the activity of nuclear SIRT1 or cytosolic SIRT2**

**(A-B)** In Panc-1 cells with *GOT2* knocking-down and putting-back, the level of indicated proteins was determined by western blotting.

Yang et al. Supplemental Figure 12

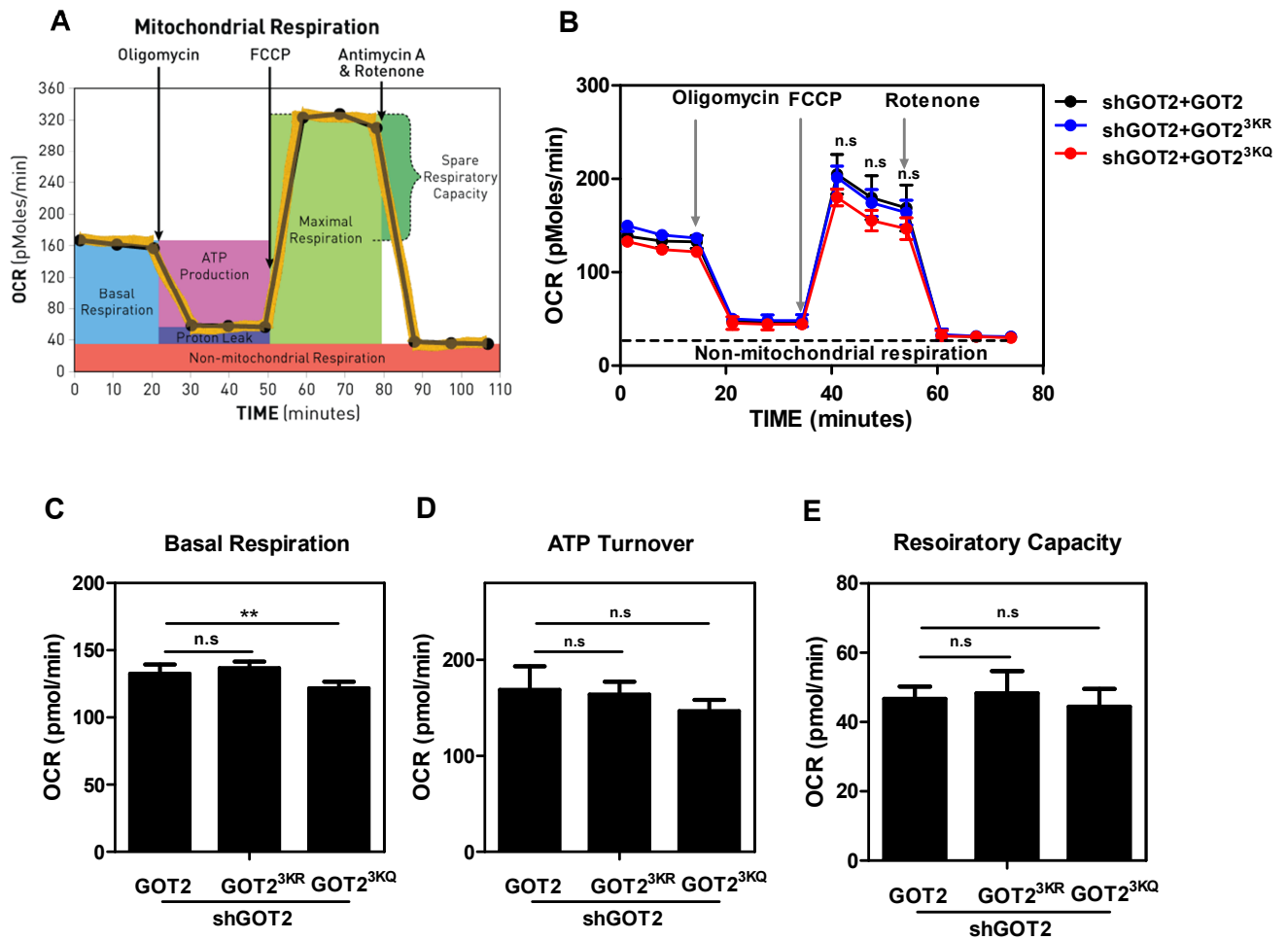


**Figure S12. GOT2 3K acetylation decreases basal respiration without affecting ATP turnover and respiration capacity in the cell**

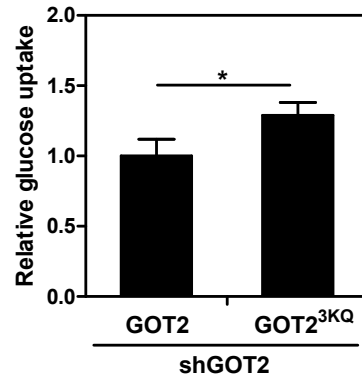
Oxygen consumption rate (OCR) was used to determine the bioenergetics profile of Panc-1 cells with *GOT2* knocking-down and putting-back using a Seahorse Bioscience XFe 96 analyzer system as described in 'Method' (as in **A**). The bioenergetics profile of rescued cells expressing wild-type *GOT2* (black circle), 3KR mutant *GOT2* (blue circle), and 3KQ mutant *GOT2* (red circle) was compared (**B**). Basal respiration, ATP turnover, and respiratory



capacity were determined by calculating average value for each phase (**C-E**). Shown are average values with standard deviation (S.D.) of triplicated experiments. \*\*denotes the  $p < 0.01$  for the indicated comparisons; n.s.= not significant.

Yang et al. Supplemental Figure 13

A



B

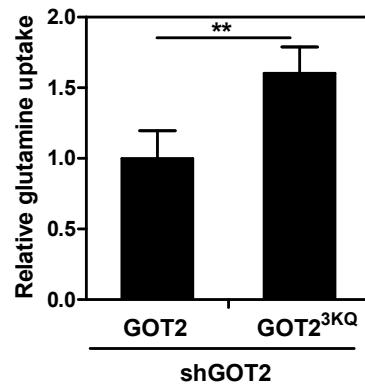


**Figure S13. GOT2 3K acetylation significantly increases glucose and glutamine uptake**

Panc-1 cells with *GOT2* knock-down and re-expression of wild-type or the 3KQ mutant *GOT2* were maintained with glucose (25 mM) or glutamine (4 mM).

The uptake of glucose and glutamine by the cell was determined as described in “Method”.

Yang et al. Supplemental Figure 14

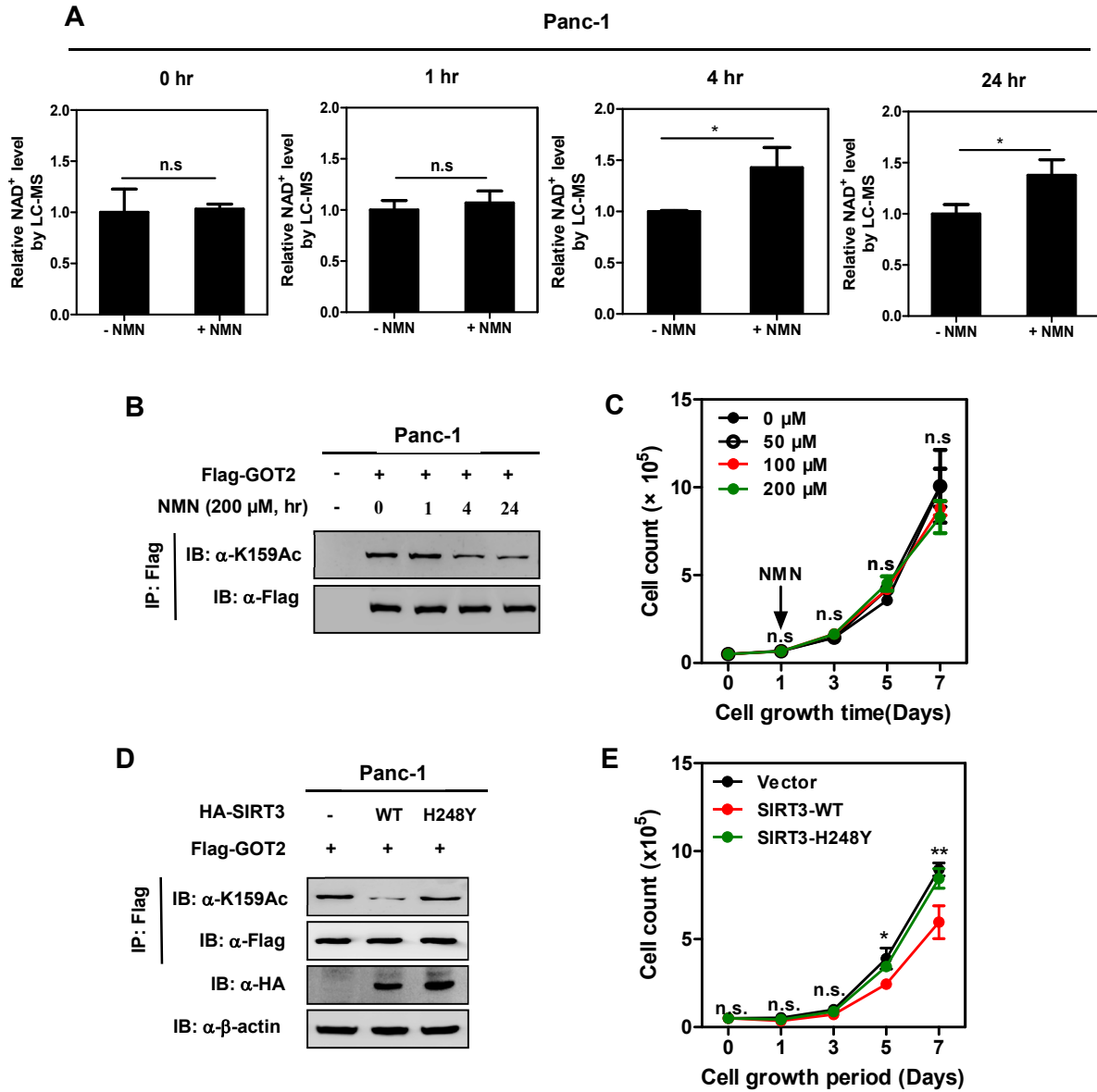


**Figure S14. Overexpression of SIRT3, but not NMN treatment, suppresses pancreatic cancer cell proliferation**

(A-B) Stable Panc-1 cells with depletion of endogenous *GOT2* and put-back of Flag-tagged wild-type *GOT2* were treated with NMN (200  $\mu$ M) for the time period as indicated, and the cellular level of  $\text{NAD}^+$  was determined by LC-MS

(A), and the K159 acetylation level of Flag-GOT2 was determined by western blot analysis (B).

**(C)** Stable Panc-1 cells with depletion of endogenous *GOT2* and put-back of Flag-tagged wild-type *GOT2* were seeded in a 6-well plate at day 0, and different concentrations of NMN were added into the cell culture medium at day 1 after seeding. NMN has been replenished to the cells every day for a period of 6 days. Cell numbers were counted every 2 days over a period of 6 days.

**(D)** Stable Panc-1 cells overexpressing Flag-GOT2 were transfected with retroviral plasmids expressing HA-tagged wild-type or catalytic inactive mutant SIRT3. The presence of ectopically expressed proteins and the K159 acetylation level of Flag-GOT2 was determined by western blot analysis.

**(E)** Stable Panc-1 cells in (D) were seeded in a 6-well plate at day 0. Cell numbers were counted every 2 days over a period of 7 days.

Shown are average values with standard deviation (S.D.) of triplicated experiments. n.s.=not significant. \*denotes the  $p < 0.05$ , \*\*denotes the  $p < 0.01$  for the indicated comparisons; n.s.= not significant.

## **Supplementary Experimental Procedures**

### **Antibodies**

Antibodies specific to GOT2 (Proteintech), SIRT3 (Cell Signaling Technology), MDH2 (Cell Signaling Technology), Phospho-Histone H3 (Ser10) (Cell Signaling Technology), Histone H3 (Cell Signaling Technology), HA (Santa Cruz) and Flag (Shanghai Genomics) were purchased commercially. The generation of pan-Acetyl-Lysine antibody was described previously (Guan et al, 2010). Polyclonal antibody to acetyl-GOT2-K159 was generated by synthesized peptide CDVFLPK(Ac)PTWGN (GL Biochem) as antigen to immunize rabbit.

### **Plasmids**

The cDNA encoding full-length human GOT2, MDH2, SIRT3, SIRT4, and SIRT5 were cloned into Flag, Myc, HA or His-tagged vectors (pcDNA-Flag; pcDNA-Myc; pcDNA3-HA; pSJ3). Point mutations of GOT2 and SIRT3 were generated by QuickChange Site-Directed Mutagenesis kit (Stratagene). The full-length human GOT2 and mutants were sub-cloned into His-pSJ3.

### **Cell culture, transfection and treatment**

HEK293T cells were cultured in Dulbecco's Modified Eagle's Medium (DMEM) (GIBCO) supplemented with 10% new born bovine serum (Biochrom, Germany), the 100 units/ml penicillin, 100 µg/ml streptomycin, and 8 mM

L-glutamine (Invitrogen). Panc-1 cells were cultured in Dulbecco's Modified Eagle's Medium (DMEM) (GRBCO) with 10% fetal calf serum (Hyclone), penicillin and streptomycin. Plasmid transfection was carried out using the calcium phosphate method or lipofectamine 2000 (Invitrogen).

Cells were treated with deacetylase inhibitors, TSA (Cell Signaling Technology) and NAM (Sigma). Moreover, chemicals which can regulate the cytosolic NADH/NAD<sup>+</sup> ratio in the cell, including AOA (TCI), Oxamate (Sangon Biotech), EGCG (TCI), were purchased commercially.

### **Animals experiments**

Male BALB/c mice (6-8 weeks of age, weighing 20-25 g) were purchased from Fudan Animal Center. Animals were given unrestricted access to a standard diet and tap water. Animal experiments were performed at Fudan Animal Center in accordance with the animal welfare guidelines.

Upon sacrifice, mouse tissues were harvested and homogenized using the TissueLyser-24 (Shanghai JingXin) in 0.5% NP-40 buffer containing protease inhibitor cocktail, and lysed on ice for 30 min for further analysis.

### **Immunoprecipitation and western blotting**

The cultured cells were lysed in ice-cold NP-40 buffer containing 50 mM Tris-HCl (pH 7.4), 150 mM NaCl, 0.1% NP-40 and protease inhibitors. The pancreatic tumor samples were homogenized using the TissueLyser-24

(Shanghai JingXin) in 0.5% NP-40 buffer containing protease inhibitor cocktail, and then were lysed at 4°C for 30 min. Cell lysate was incubated with Flag beads (Sigma) for 3hr at 4°C. Flag, HA and Myc western blotting was blocked with 5% fat-free milk (BD Biosciences). For acetylation western blotting, 50 mM Tris (pH 7.5) with 10% (V/V) Tween-20 and 1% peptone (Sigma) was used for blocking. Primary and secondary antibodies are prepared with 5% fat-free milk and 50 mM Tris (pH 7.5) with 0.1% peptone, respectively.

### **Measurement of intracellular ATP**

Intracellular ATP concentration was measured by using an ATP assay kit (Beyotime). In brief, 200 µl of cell suspension was centrifuged at 1,200× g for 5 min. 100 µl supernatant and 100 µl luciferin–luciferase reagents were mixed for 2 sec at least. Luminescence was monitored by using a Modulus™ Micoplate Reader. The protein concentration was determined by BCA Protein assay kit (Beyotime). The signal intensity was normalized by cell protein levels and showed as relative ATP levels.

### **Measurement of intracellular NADPH and NADP<sup>+</sup>**

The intracellular levels of NADPH and NADP<sup>+</sup> were measured by enzymatic cycling methods as previously described (Wagner & Scott, 1994; Zerez et al, 1987). In brief, 1.5×10<sup>6</sup> cells were seeded in 10 cm dishes. On the next day, cells were lysed in 400 µL of extraction buffer (20 mM NAM, 20 mM NaHCO<sub>3</sub>, 100 mM Na<sub>2</sub>CO<sub>3</sub>) and centrifuged at 1,200 × g for 15 min. For NADPH extraction, 150 µl of the supernatant was incubated in a heating block for 30

min at 60°C. 160 µl of NADP-cycling buffer (100 mM Tris-HCl, pH8.0; 0.5 mM thiazolylblue; 2 mM phenazine ethosulfate; 5 mM EDTA) containing 1.3 U of G6PD was added to a 96-well plate containing 20 µl of the cell extract. After incubation for 1 min at 30°C in darkness, 20 µl of 10 mM G6P was added to the mixture, and the change in absorbance at 570 nm was measured every 30 sec for 10 min at 30°C in a SpectraMax M5 Microplate Reader (Molecular Devices). All the samples were run in triplicate. The concentration of NADP<sup>+</sup> was calculated by subtracting NADPH (heated sample) from the total of NADP<sup>+</sup> and NADPH (unheated sample).

#### **Measurement of mitochondrial NADH and NAD<sup>+</sup>**

For mitochondrion isolation, cells ( $5 \times 10^6$ ) were homogenized in 500 µl of ice-cold HEPES buffer (20 mM HEPES, 250 mM sucrose, 10 mM KCl, 1.5 mM MgCl<sub>2</sub>, 1 mM EDTA, 1 mM EGTA, PH 7.4 ). Leave on ice for 20 min. The homogenate was centrifuged at  $600 \times g$  for 15 min at 4°C. Then the supernatant was centrifuged at  $12,000 \times g$  for 10 min at 4 °C. The pellet was resuspended in 1 ml of the HEPES buffer and centrifuged  $12,000 \times g$  for 10 min at 4 °C. Discard the supernatant, and the pellet was resuspended with 400 µl of extraction buffer (20 mM NAM, 20 mM NaHCO<sub>3</sub>, 100 mM Na<sub>2</sub>CO<sub>3</sub>), and centrifuged at  $1,200 \times g$  for 15 min.

For NADH extraction, 150 µl of the supernatant was incubated in a heating block for 30 min at 60°C. 160 µl of NAD-cycling buffer (100 mM Tris-HCl, pH 8.0; 0.5 mM thiazolylblue; 2 mM phenazine ethosulfate; 5 mM EDTA) containing 1.3 U of alcohol dehydrogenase was added to a 96-well plate containing 20 µl of the mitochondria extract. After incubation for 1 min at



30°C in darkness, 20 µl of 100 % ethanol was added to the mixture, and the change in absorbance at 570 nm was measured every 30 sec for 10 min at 30°C in a SpectraMax M5 Microplate Reader (Molecular Devices). All the samples were run in triplicate. The concentration of NAD<sup>+</sup> was calculated by subtracting NADH (heated sample) from the total of NAD<sup>+</sup> and NADH (unheated sample).

### **Measurement of intracellular GSSG, GSH, and NAD<sup>+</sup>**

Intracellular GSSG, GSH, and NAD<sup>+</sup> levels were determined by using liquid chromatography–mass spectrometry (LC-MS/MS). In short, cells were harvested by using 80% (v/v) pre-cold (-80°C) methanol and centrifuged at 4 °C at 12000 rpm for 15 min. The supernatants were then subjected to LC-MS analysis using a Shimadzu LC (LC-20AB pump) system coupled with 4000 qtrap triple quadrupole mass spectrometer (AB sciex). A Phenomenex NH2 column (50mm×2.0mm I.D., 5 µm particle size, 100Å) was used. The mass spectrometer was optimized and set up in selected reaction monitoring (SRM) scan mode for monitoring the [M-H]<sup>-</sup> of GSSG (m/z 611.6→306.2), GSH (m/z 306.2→142.8), and NAD<sup>+</sup> (m/z 662.3→540.1). The Analyst Software was used for analysis.

### **Measurement of intracellular ROS**

Intracellular ROS production was determined by using a fluorescent dye 2', 7'-dichlorofluorescein diacetate (H<sub>2</sub>DCF-DA, Sigma). Briefly, cells were washed with PBS and incubated with 10 µM H<sub>2</sub>DCF-DA at 37°C for 30 min to load the fluorescent dye. Cells were washed twice with PBS and trypsinized for

menadione treatments. Fluorescence (Ex.488nm, Em.525nm) was monitored by a SpectraMax M5 Microplate Reader (Molecular Devices).

#### **Measurement of cytosolic redox status**

Redox-sensitive green fluorescent protein 1 (roGFP1) was adopted to measure the thiol-disulfide metabolic state in living cells (Dooley, 2004). In short, cells stably expressing roGFP1 were harvested by trypsinization, following re-suspension in PBS. Fluorescence (Ex.400/485nm, Em.525nm) was monitored by a SpectraMax M5 Microplate Reader (Molecular Devices).

#### **Measurement of cell respiration**

The oxygen consumption rate (OCR) was determined in cell extracts as described previously (Viale et al, 2014). In brief,  $2 \times 10^4$  cells were seeded in a 96-well culture plate from SeaHorse Bioscience (Billerica, MA) and incubated for 24 hours. During respirometry, wells were sequentially injected at the indicated times with: oligomycin (Oligo, 1  $\mu$ M), an inhibitor of ATP synthase, to assess respiration required for ATP turnover; carbonyl cyanide p-[trifluoromethoxy]-phenyl-hydrazone (FCCP, 0.5  $\mu$ M), an uncoupler of electron transport, to induce maximal respiration; Rotenone was then added at a final concentration of 1.0  $\mu$ M to inhibit electron transport and measure non-mitochondrial respiration.

#### **Flow cytometry**

Cell apoptosis was determined by using a commercial FITC Annexin Apoptosis Detection Kit (BD Pharmingen). Briefly, cells were washed twice with cold PBS

and then resuspended in  $1 \times$  binding buffer at a concentration of  $1 \times 10^6$  cells/ml. 5  $\mu$ l of FITC Annexin V and 5  $\mu$ l propidium iodide (PI) were added into the 100  $\mu$ l of the solution ( $1 \times 10^5$  cells). Cells were then incubated for 15 min at 25°C in the dark. The percentages of Annexin V and/or PI-positive cells were determined by flow cytometer (BD Accuri™).

### **Immunohistochemistry (IHC)**

Paraffin-cut sections of xenograft tumors (5  $\mu$ m) were prepared, and cell proliferation was assessed by performing immunohistochemical staining using an antibody against PCNA (Cell Signaling) as previously described (Yang et al, 2013).

### **Supplementary Reference**

Guan KL, Yu W, Lin Y, Xiong Y, Zhao S (2010) Generation of acetyllysine antibodies and affinity enrichment of acetylated peptides. *Nat Protoc* 5: 1583-1595

Viale A, Pettazzoni P, Lyssiotis CA, Ying H, Sánchez N, Marchesini M, Carugo A, Green T, Seth S, Giuliani V (2014) Oncogene ablation-resistant pancreatic cancer cells depend on mitochondrial function. *Nature* doi:10.1038/nature13611

Wagner TC, Scott MD (1994) Single extraction method for the spectrophotometric quantification of oxidized and reduced pyridine nucleotides in erythrocytes. *Anal Biochem* 222: 417-426

Yang H, Liu Y, Bai F, Zhang JY, Ma SH, Liu J, Xu ZD, Zhu HG, Ling ZQ, Ye D, Guan KL, Xiong Y (2013) Tumor development is associated with decrease of TET gene expression and 5-methylcytosine hydroxylation. *Oncogene* 32: 663-669

Zerez CR, Moul DE, Gomez EG, Lopez VM, Andreoli AJ (1987) Negative modulation of Escherichia coli NAD kinase by NADPH and NADH. *J Bacteriol* 169: 184-188